



Extended Absolute Fuzzy Connectedness Segmentation Algorithm Utilizing Region and Boundary-Based Information

T. H. Farag^{1,2}  · W. A. Hassan^{1,2} · H. A. Ayad² · A. S. AlBahussain³ · U. A. Badawi¹ · M. K. Alsmadi¹ 

Received: 28 November 2016 / Accepted: 8 May 2017 / Published online: 29 May 2017
© King Fahd University of Petroleum & Minerals 2017

Abstract Image segmentation is the process of dividing an image into meaningful objects to perform different analysis operations. Fuzzy connectedness (FC)-based segmentation methods usually give robust segmentation results; on the other hand, they suffer from some weaknesses. The generalized or absolute fuzzy connectivity (GFC) segmentation method is the foundation of most FC-based methods. This method has two apparent weaknesses: It combines different objects in the case of their boundaries are blurred, and it can not find the object of interest if the threshold value determined without interactive manner. In this manuscript, we introduce extensions to the GFC algorithm to tackle the mentioned weaknesses. The FC and affinity functions in the extended algorithm utilize region- and boundary-based information to overcome the first weakness. Moreover, this algorithm suggests a near optimal threshold generated automatically to

eliminate the need for any interaction. Comparisons has been made to quantitatively evaluate the proposed algorithm over a three sorts of data set of scenes. Measures of relevance have been calculated for two data sets. Results indicate improved segmentation accuracy and also showed that the weaknesses of the traditional GFC algorithms have been eliminated to some extent.

Keywords Image segmentation · Fuzzy connectedness · Algorithms · Optimal thresholds · Hybrid base segmentation

1 Introduction

Image segmentation is considered an essential operation to perform image analysis since by which the representation as an image becomes more meaningful and easier to analyze. Segmentation methods can be classified into two major categories depending on the dominated features they utilize, namely region- and edge-based methods [1]. Region-based methods divide an image into homogeneous areas while boundary-based methods extract contours that usually separate different object areas [2,3]. A recent category of hybrid segmentation methods exploits both properties to produce more effective segmentations [4]. Segmenting objects within an image in a hard manner (binary labeling) could produce inefficient results. In a different manner, image segmentation can be carried out by implementing some fuzzy rules to address the image uncertainties such as FC-based methods. An FC-based segmentation method is a region-based method that attempts to describe the segmentation task with fuzzy rules [5,6]. Some of these rules are concerned with the similarity of image pixels and the distance among them. FC-based segmentation methods such as generalized, relative and iterative relative methods have the advantage of robustness with

✉ T. H. Farag
tamer@sci.cu.edu.eg
W. A. Hassan
wahassan@uod.edu.sa
H. A. Ayad
ahassan@sci.cu.edu.eg
U. A. Badawi
ubadawi@uod.edu.sa
M. K. Alsmadi
mkalsmadi@uod.edu.sa

¹ College of Applied Studies and Community Service, University of Dammam, Dammam, Kingdom of Saudi Arabia
² Department of Mathematics, Faculty of Science, Cairo University, Giza, Egypt
³ College of Medicine, University of Dammam, Dammam, Kingdom of Saudi Arabia

seed selection over other most region-based methods [7, 8]. These methods do not attempt to use in its framework prior shape and appearance knowledge about object boundaries [9, 10]. In case of missing information about certain segments of the object boundaries, FC-based segmentation methods often could merge the object of interest with other objects surrounding it [9, 10]. In the literature, ([8, 11, 12]) researchers try to handle the weakness of poorly defined boundaries by combining FC-based methods with other segmentation methods such as Voronoi diagram (VD), deformable models (DM) and graph cut (GC) into a hybrid single segmentation framework. These methods have a control over the object boundaries better than FC-based methods [12]. However, they have their own weakness properties that are considered as a challenge for the hybrid method of segmentation. Some of these methods require an extra interaction behavior from the user and/or increase the general cost of running of the segmentation problem. GFC method is considered as the basic FC-based method [13]. It has to select an appropriate threshold value to complete the segmentation process. GFC method generally suffers from the weakness of threshold value selection [10].

In this proposal, new modifications on the traditional GFC algorithm have been introduced to overcome the previously mentioned weakness points. Our algorithm is a hybrid (edge and object) method that utilizes an edge operator to detect the location of variations between objects at which characteristics of pixels are gathered. Furthermore, it employs a membership function formula of affinity, which reflects the connectedness between adjacent spels, to make FC capable of reducing the leaking weakness through boundaries. In addition, the algorithm introduces an automatic procedure to select an appropriate threshold value.

In Sect. 2, the principles of fuzzy connectedness are described briefly. In Sect. 3, the algorithm that shows our main contributions—illustrated in the above discussion—is described. In Sect. 4, the data set used for the evaluation process is defined, and evaluation rules that measure the efficiency of the proposed algorithm are presented. In Sect. 5, a comparison experiment that is performed to evaluate our algorithm and display the obtained results provided with many graphic plots is discussed. In Sect. 6, the conclusion is presented.

2 Principles

Let \mathcal{C} be a 2D image scene, a fuzzy connected object in \mathcal{C} is recognized as a subset of adjacent and joined spels (pixels) of the scene, which are highly fuzzy connected. Fuzzy connectivity among spels of a scene is evaluated in terms of both fuzzy adjacency and fuzzy affinity, which reflect how many spels are close in space and how many have similar qualities, respectively.

Fuzzy adjacency membership function, denoted μ_α , of the fuzzy adjacency relation α , assigns a value in the unit interval to a pair of spels depending on how much they are adjacent to each other. The larger the distance between them is, the lower the value will be.

Fuzzy affinity membership function, denoted μ_k , of the fuzzy affinity relation α , assigns a value in the unit interval to a pair of spels depending on how much the two spels hang together in the scene. In order to describe this relation, two relations are considered beside the adjacency relation. These are the homogeneity and object-based relations, denoted by ψ and ϕ , respectively.

The membership functions of these relations, denoted by μ_ψ and μ_ϕ , respectively, assign a value in the unit interval to a pair of spels in a given scene \mathcal{C} depending on, how much the two spels are similar to each other and to their object features, respectively. Hence, a general formula for μ_k could be as follows,

$$\mu_k(c, d) = h(\mu_\alpha(c, d), \mu_\psi(c, d), \mu_\phi(c, d)) \quad (2.1)$$

where the constraints on h are described in [14]. An example of μ_k as proposed in [14] is,

Let c, d be two spels in a scene \mathcal{C} including an object o and a background b . Let o has the statistics k_ψ, k_o and m_o of its spels, representing standard deviation of differences of intensities, standard deviation of intensities and mean of intensities, respectively. Let b has the statistics k_b and m_b that are analogous to k_o and m_o for its spels. We consider the formulation for μ_k as to be

$$\mu_k(c, d) = \mu_\alpha(c, d) \sqrt{\mu_\psi(c, d) \mu_\phi(c, d)}, \quad (2.2)$$

where the fuzzy adjacency membership function is

$$\mu_\alpha(c, d) = \begin{cases} \frac{1}{1+z \left(\sqrt{\sum_{i=1}^2 (c_i - d_i)^2} \right)}, & \text{if } \sum_{i=1}^2 |c_i - d_i| \leq 2 \\ 0, & \text{otherwise} \end{cases} \quad (2.3)$$

where z is a nonnegative constant. And the fuzzy homogeneity membership function is

$$\mu_\psi(c, d) = e^{-\frac{|f(c) - f(d)|}{2K_\psi^2}}, \quad (2.4)$$

and the fuzzy object-based membership function is

$$\mu_\phi(c, d) = \begin{cases} 1, & \text{if } c = d \\ \frac{\mathcal{W}_o(c, d)}{\mathcal{W}_o(c, d) + \mathcal{W}_b(c, d)}, & \text{if } \mathcal{W}_o(c, d) \neq 0 \\ 0, & \text{otherwise} \end{cases} \quad (2.5)$$

where

$$\mathcal{W}_o = \underbrace{\min[W_o(f(c)), W_o(f(d))]}_{\text{Object Component}} \times \underbrace{\mathcal{W}_b = \max[W_b(f(c)), W_b(f(d))]}_{\text{Background Component}}, \tag{2.6}$$

$$W_o(x) = e^{-\frac{(x-m_o)^2}{2K_o^2}}, \quad W_b(x) = e^{-\frac{(x-m_b)^2}{2K_b^2}} \tag{2.7}$$

A non-empty path p_{cd} in a scene \mathcal{C} from a spel $c \in C$ to a spel $d \in C$ is a sequence $\langle c^{(1)}, c^{(2)}, \dots, c^{(m)} \rangle$ of $m > 2$ spels, all in C , such that $c^{(1)} = c$ and $c^{(m)} = d$.

Fuzzy connectedness (FC) membership function, μ_K , of the fuzzy connectedness relation, K , reflects the strength of connectedness between any pair of spels in the scene. In order to compute $\mu_K(c, d)$, each path connecting them should be considered and its connectedness should be evaluated as well. Each successive pair of spels constitutes a link that has a strength value which is the affinity between the pair spels. As each path composes a chain of links, we assign its strength value to be the smallest pairwise spel affinity along the path (the weakest link). After assigning all paths strengths, the connectedness between c and d is the strongest of them.

Fuzzy connectedness scene is a scene in which each spel represents the strength of connectedness between that spel and a seed spel chosen inside the scene.

Fuzzy connected object, denoted as \mathcal{O} , of strength θ consists of all spels $c \in C$ containing a seed spel $o \in C$ such that $\mu_K(c, o) > \theta$.

3 Methods

The main goal of the traditional GFC-based algorithm in [15] (GFC) is to generate an FC scene with respect to a specified seed spel within an object, needed to be segmented, of a given scene. This FC scene should contain a fuzzy connected object to the threshold in a further step. Fuzzy affinity is the principal component in the definition of FC. In the literature, the formulation of affinity usually utilizes information about the object and its background as given in Eqs. 2.4, 2.5. The main goal of our modified algorithm is to extend the target regions from which the affinity utilizes its information, to include the boundary region located between both object and background regions. The rationale of incorporating boundary-based information is to make affinity respond with low values to the boundary spels. Thus, it is expected that FC of background spels to the seed spel will drop in value as a result. Consequently, the resulting FC scene keeps a distinctive difference between the spels in object and background regions.

For the results presented within this paper, the affinity formulation of Eq. 2.2 has been utilized with adding a new component to respond to boundary information in μ_ϕ to be

$$\mu_\phi(c, d) = \begin{cases} 1, & \text{if } c = d \\ \frac{a_1 \mathcal{W}_o(c,d)}{a_1 \mathcal{W}_o(c,d) + a_2 \mathcal{W}_b(c,d) + a_3 \mathcal{W}_e(c,d)}, & \text{if } \mathcal{W}_o(c, d) \neq 0 \\ 0, & \text{otherwise} \end{cases} \tag{3.1}$$

where a_1, a_2 and a_3 are constants used to weight $\mathcal{W}_o, \mathcal{W}_b$ and \mathcal{W}_e according to their relative importance,

$$\mathcal{W}_e = \underbrace{\max[W_e(f(c)), W_e(f(d))]}_{\text{Boundary Component}}, \tag{3.2}$$

$$W_e(x) = e^{-\frac{(x-m_e)^2}{2K_e^2}} \tag{3.3}$$

where K_e and m_e are analogous to K_o and m_o for the boundary region.

In the following, a detailed description of the proposed extension will be presented. It consists of two algorithms. Algorithm one is to build up a fuzzy segmented scene. Hence, the final segmentation is based on selection of a proper threshold. This threshold in GFC method generally is selected by the human interaction. However, Algorithm two presents automatic steps to let the method itself to determine a proper threshold.

3.1 Extended FC

In the following, the first portion of the modified proposed method, which builds up image fuzzy segmentation extended based on the traditional GFC algorithm, is presented. This part of the algorithm aims to resolve the weakness of leaking through boundaries, which has been stated. It generates an FC scene for a given scene to be segmented based on a proper threshold, which will be shown by the second algorithm portion revealed later.

Input: $\mathcal{C} = (C, f)$ scene, seed spel $s \in C$

Output: \mathcal{C}_s FC scene with respect to s

begin

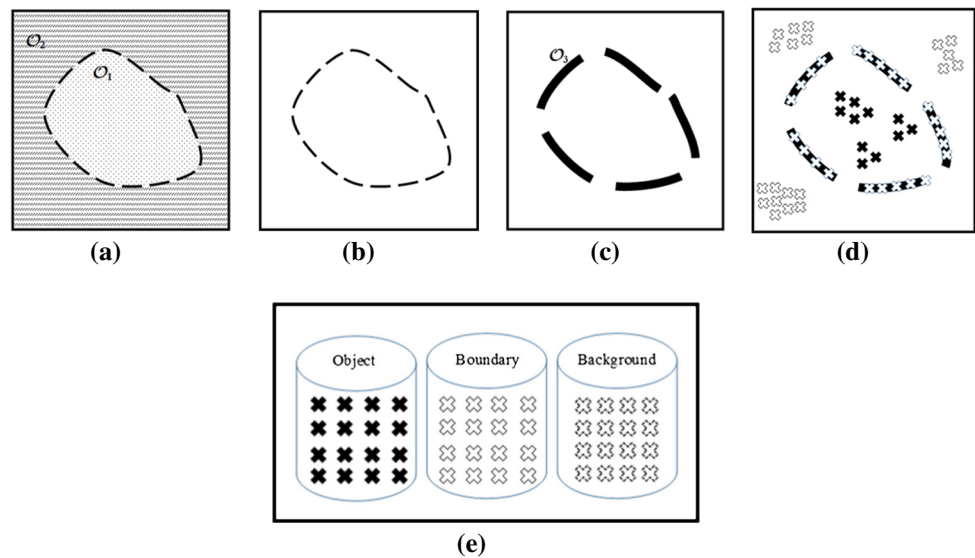
- Select sample areas of spels within object, boundary and background regions of \mathcal{C} ;
- Calculate the *mean* and *standard deviation* statistics for the selected spels of relative regions;
- Implement *kFOE* algorithm in [15] with affinity in Eq. 2.2 with replacing Eq. 2.5 with Eq. 3.1 to output \mathcal{C}_s ;

end

Algorithm 1: Fuzzy Connectedness Scene

In Line 1, since it is more practical to select spels from object and background regions rather than selecting it from the boundary region, we have implemented that using Sobel’s

Fig. 1 **a** A scene with object \mathcal{O}_1 and a background \mathcal{O}_2 in which the object boundary has poorly defined edge segments represented by the gaps in the boundary contour. **b** It is the edge map detected by Sobel's edge operator, in which portion of the edge is successfully extracted while missing portion of the edge could not be detected. **c** Expanded edge segments which include all edge spells and its neighborhood spells. **d** Spells that are selected from different regions. These spells are illustrated by coded x symbols listed in **(e)**



edge operator. First, this operator is applied at the input scene to detect edge segments. Then, we expand along these segments to include the neighborhood of spells which are the closest to the edge spells as shown in Fig. 1c. From these spells, the boundary region is defined, or in other words, the spells that probably have the edge features.

3.2 Automatic Threshold Selection

After implementing the first algorithm portion in 1, an FC scene, denoted \mathcal{C}_s , is generated. In order to complete the segmentation of the input scene, denoted \mathcal{C} , a thresholding step on \mathcal{C}_s is required. The second algorithm portion in 2 proposes an automatic procedure for selecting an appropriate threshold. Therefore, this completes the segmentation process and also handles the second kind of weakness regarding GFC method.

Input: $\mathcal{C}, \mathcal{C}_s$

Output: \mathcal{C}_b segmented scene of \mathcal{C}_s

begin

- 1) Apply Canny edge operator on \mathcal{C} to generate an edge map \mathcal{C}_e that has edge and non-edge spells;
- 2) Count the occurrences of the values of connectedness of spells in \mathcal{C}_s that correspond the edge spells in \mathcal{C}_e ;
- 3) Choose the value with the second most occurrence as the threshold value t ;
- 4) Threshold the scene \mathcal{C}_s with t threshold and output the binary scene \mathcal{C}_b as the segmented scene;

end

Algorithm 2: Auto Segmentation Algorithm

Line 3 of Alg. 2 uses the second most occurring value as the threshold value since the first most occurrence value almost corresponds to the clutter of edge segments caused by noise effect.

In Fig. 2a, sample scene and its connectivity are shown in Fig. 2a, b, respectively, and Fig. 2c–e illustrates three thresholded scenes of the connectedness scene at three different threshold values. Figure 2f is the result of step in line 1 and the step in line 3 is performed in Fig. 2g. After applying the step in line 3, we have t as the proposed threshold. Figure 2h shows the thresholded binary scene (segmented scene) by t threshold of the connectedness scene.

4 Data Set and Evaluation

4.1 Data Set

For evaluation purpose, we used three data sets. First data set consists of 75 images. These images have been derived from the atlas of the human brain [16, 17]. Five 2D scenes are extracted from a 3D scene from the atlas. One of these scenes is shown in Fig. 3a. For each scene, the white matter region is manually separated into a new scene. Further, two constant gray levels (intensities) have been assigned to that region and its background. Based on the five white matter scenes, our data set is formed through affecting them by different blur and noise levels.

To build up an image with boundary leaks, apply blurring effect on the image is one way. Hence, blurring will decrease the differences between the pixels, including the border, and that may do some leaks in the border. Another way is to apply so noise to the image, because affect getting right separation of any object in an image. Here, the selected scenes will be blurred, noised or blurred and then noised. In the case of applying noise and blur, blur has been applied first because the selected Gaussian blur can reduce or remove the effect of the noise.

Fig. 2 A sequence of scenes that illustrate the steps of Algorithm No. 2

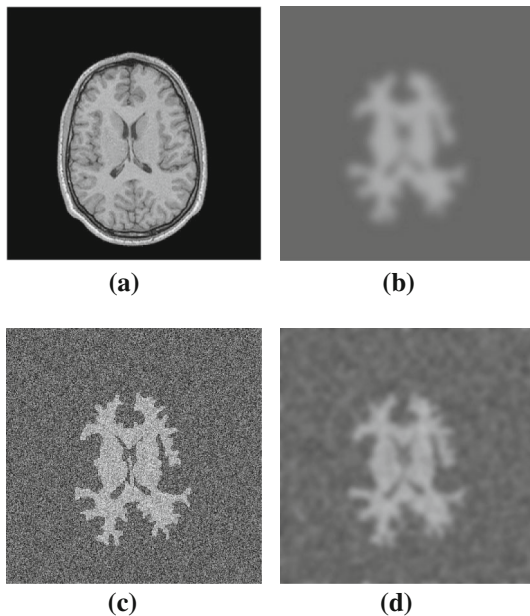
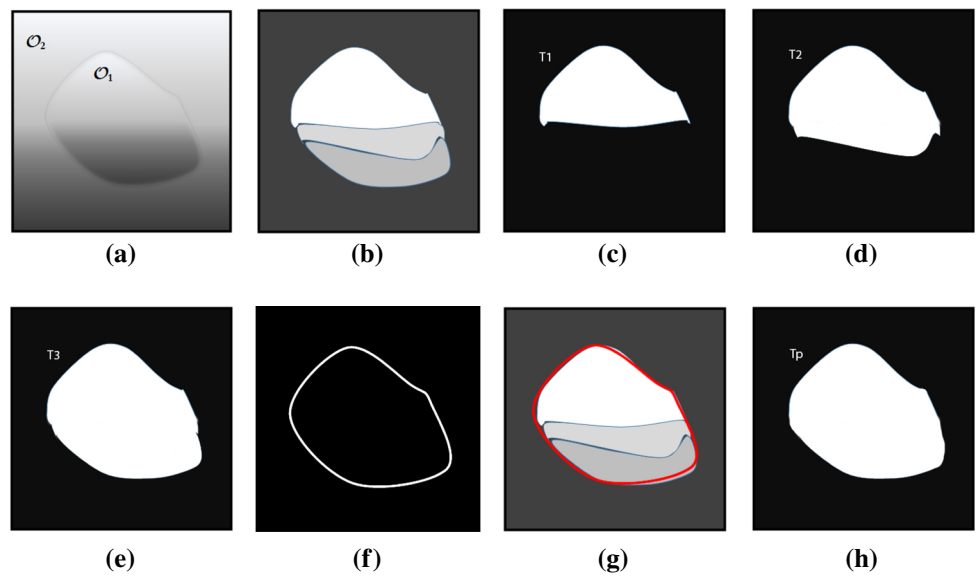


Fig. 3 **a** A 2D brain scene from the atlas of the human brain. **b** A blurred white matter scene. **c** A noisy white matter scene. **d** A blurred noisy white matter scene

For each white matter scene, four blurred scenes are generated by blurring with Gaussian filter with parameters: σ (standard deviation) = {2,4,6,8} and filter size (hsize) = {7,11,15,19}, respectively. Further, for each scene, we create five noisy scenes using zero-mean Gaussian noise with parameter: variance = {0.02,0.04,0.06,0.08,0.1}. Also, six blurred noisy scenes are produced for each white matter scene (each scene is affected with two degrees of noise and then blurred at three different degrees of blurring). Figure 3b–d shows sample scenes of blurred, noisy and blurred noisy scenes, respectively. Ultimately, the set of 20 blurred

scenes, 25 noisily scenes and 30 blurred noisily scenes are considered to be our first data set used for evaluation purpose.

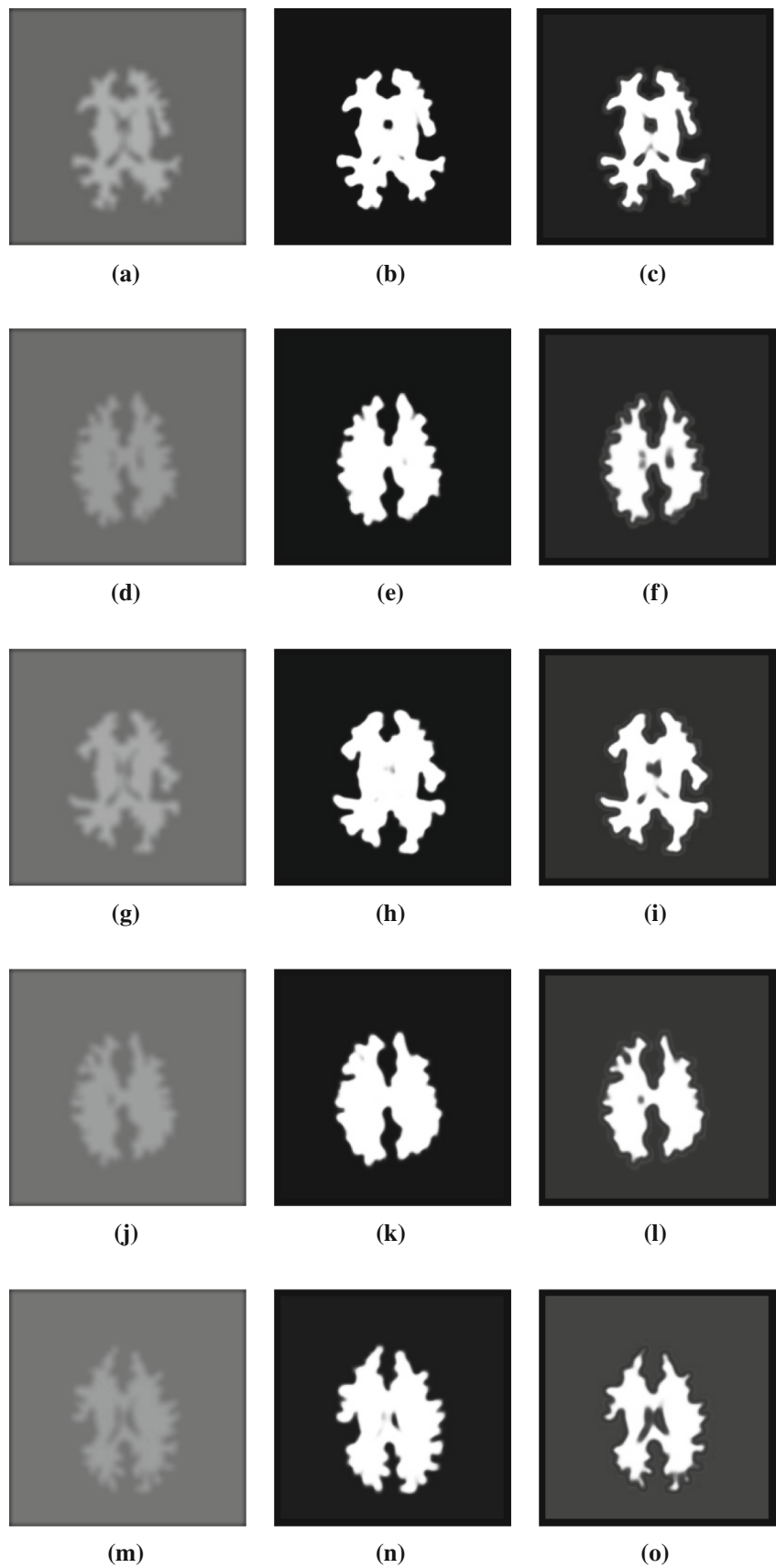
For further verification, a widely used image segmentation database has been used as the source of the second data set, which is the Internet Brain Segmentation Repository (IBSR) (<http://www.cma.mgh.harvard.edu/ibsr/>), an online database of head MR images of more than 40 subjects along with truth models for their segmentation, an example from that data set is shown in Fig. 9a.

A third set is a satellite image that shows three major observations: wadis, granite rocks and meta-volcanic rocks. This image represents the field of Gabal El Mueilha and the surrounding area; Gabal El Mueilha is located in the Idfu-Marsa Alam area, Central Eastern Desert, Egypt. El Mueilha area consists of post-collision granitic rocks intruding Pan-African metasediments, metavolcanics and granodiorites [18]. Since the Wadis is spread over the whole image breaking the mass rocks into many rock segments, we had to extract each rock segment as a single object from the image and recombine all these segments into a unified segmented image. Figure 10a shows the satellite image with red dots that locate the seed representative points for rock segments. For each rock segment, we provide location of a seed pixel along with estimation of parameters for the segment area pixels into the proposed segmentation algorithm.

4.2 Evaluation

For evaluation of the proposed algorithm, it is needed to assess both Algs. 1 and 2. Basically, it is needed to figure out how much the boundary component in Eq. 3.1 affects the segmentation of image scenes and eliminates the first kind of weakness of traditional GFC method and, in addition,

Fig. 4 In each row above, three scenes expressing a data set scene, connectivity scene generated by the original method and a connectivity scene generated by the proposed method are displayed in order



how much the proposed threshold in Alg. 2 behaves like an optimal threshold and eliminates the second kind of weakness. We will follow a quantitative evaluation procedure that has been utilized in [14, 19] to address the previous issues. The key idea behind this procedure is to calculate the degree of matching between a ground of truth scene C_g , usually, a binary scene and any two candidate segmented scenes, say C_{b1} and C_{b2} of scenes having C_g as their ground of truth. Thus, we can judge whether of these segmented scenes is better than the other. Consider the following formula to compute the percentage of degree of matching between two binary scenes, C_g and C_{b1} , that have equal size,

$$\text{degMatch} = \left[\left(1 - \frac{|C_g \oplus C_{b1}|}{|C_g|} \right) \times 100 \right] \quad (4.1)$$

where $|C_g|$ is the cardinality of C_g , $C_g \oplus C_{b1}$ is a binary scene yielded by the exclusive or operation (XOR) \oplus between the two binary scenes C_g , C_{b1} and $|C_g \oplus C_{b1}|$ represents the number of spels whose values are 1 (spels that have similar values in both C_g , C_{b1}).

For the first issue regarding the boundary component, a comparison has been made between segmented scenes of the data set of scenes shown above in case of implementing a GFC algorithm with the affinity formula presented in Sect. 3 (*original method*) and the proposed algorithm in Algs. 1 and 2 (*proposed method*). The resulting segmented scenes by both methods are binary scenes, since they are thresholded. Thus, the comparison between corresponding segmented scenes could be completed utilizing Eq. 4.1 considering the set of white matter region scenes as the ground of truth to our data set scenes.

For the second issue regarding the threshold parameter, we compare between the obtained threshold from Alg. 2, referred to by “*proposed threshold*” with two other thresholds, referred to by “*poorest threshold*” and “*optimal threshold*,” respectively. These thresholds are assumed to give the worst and best segmentations for their FC scenes. For a given FC scene within a data set scene, the “*poorest threshold*” and “*optimal threshold*” are identified via quantizing, at first, this scene to have a range of ten intensity values among which the user may select a threshold. For each intensity value of the ten, the FC scene under consideration is thresholded to generate a segmented scene. Then the degree of the match between the segmented scene and the corresponding ground of truth scene based on Eq. 4.1 is calculated. Ultimately, we select the threshold value with the minimum (degMatch) degree of match to be the “*poorest threshold*” among all tested 10 mating values and the “*optimal threshold*” is vice versa.

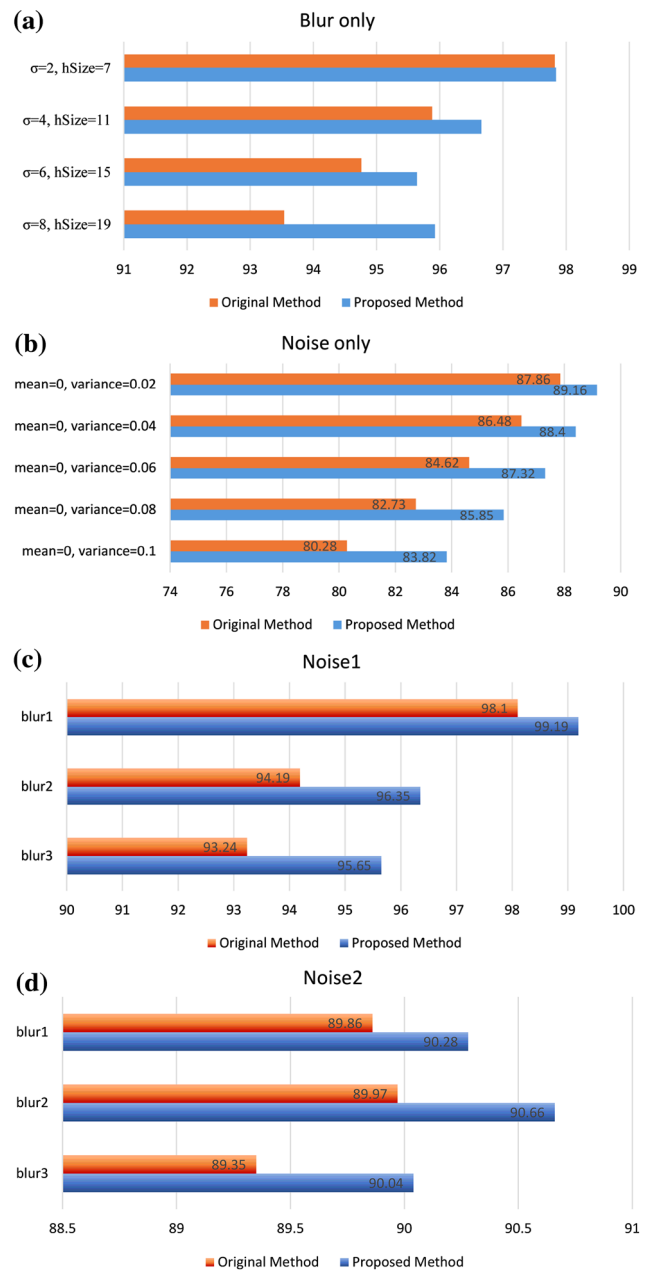


Fig. 5 Mean of evaluated matching percentage for both the original and proposed methods for the blurred (a), noisy (b) and blurred noisy (c, d) data sets

Finally, the typical measures precision, recall, F-measure and accuracy are calculated, and the proposed algorithm with the original GFC algorithm has been compared.

However, for the satellite image, a comparison between the ground of truth image for the satellite image and the segmented image by the proposed method was made that can estimate the efficiency of the proposed method.

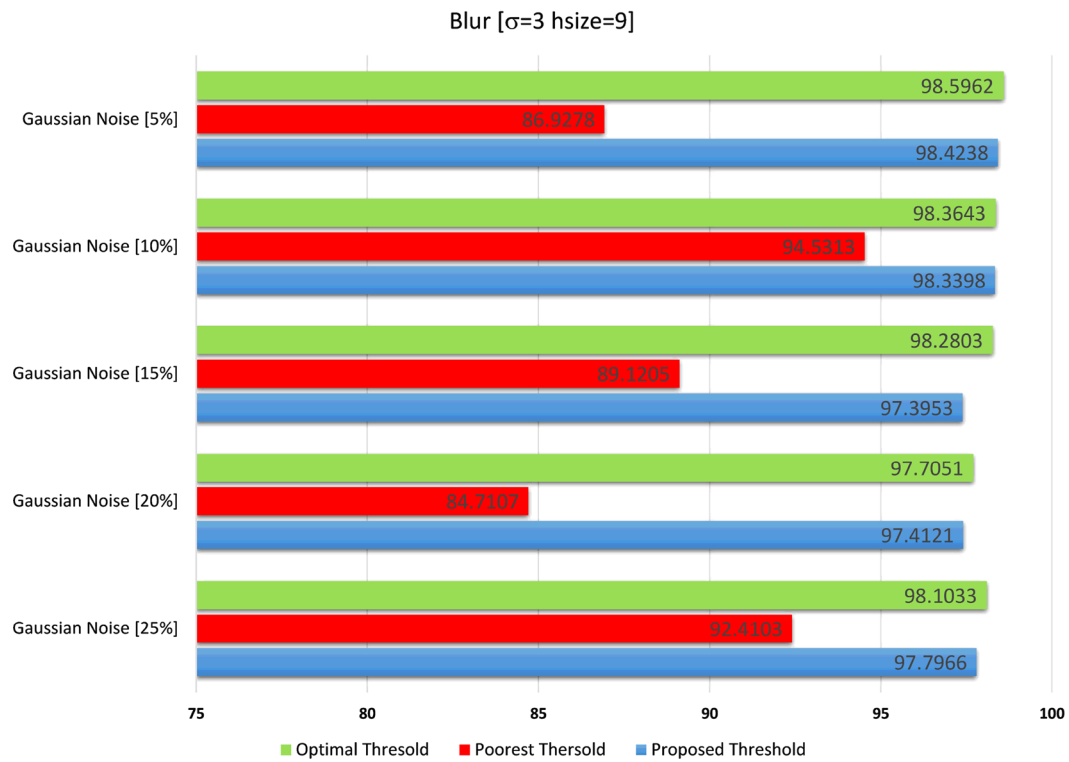


Fig. 6 Mean of evaluated matching percentage for the three thresholds (poorest threshold, proposed threshold and optimal threshold) for the blurred noisy data set

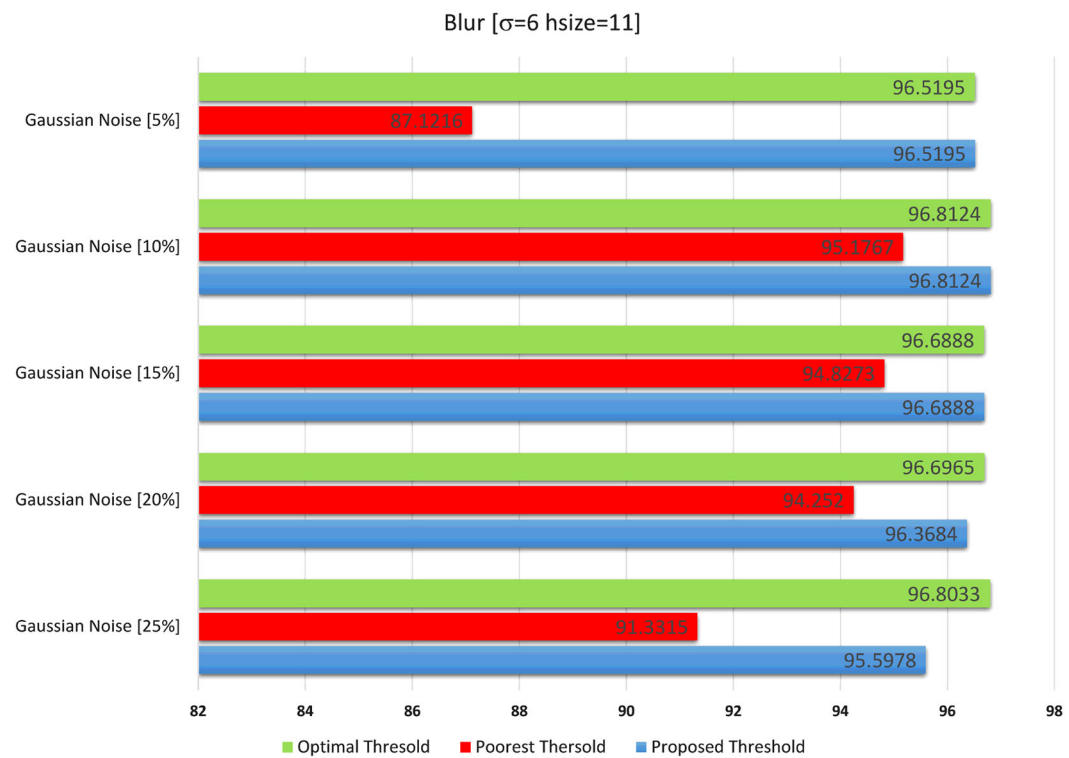


Fig. 7 Analogous to Fig. 6 for different blurred noisy data set scenes

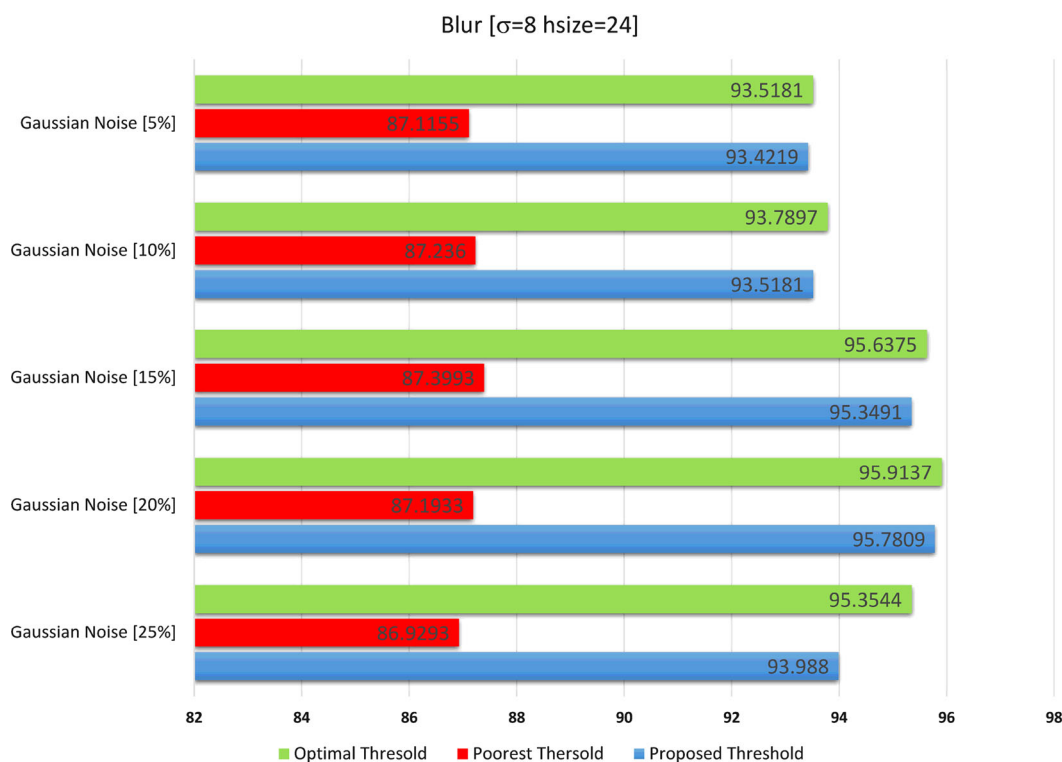


Fig. 8 Analogous to Fig. 6 for different blurred noisy data set scenes

5 Results

5.1 Original Versus Proposed

The first comparison has been made between “original method” and “proposed method.” We apply both methods to the data set to generate segmented scenes; then, we assign for each scene a degree of match determined by Eq. 4.1. For each kind of scenes in the data set (blurred, noisy, blurred noisy), the average degree of matching or AVM for both methods has been calculated. Figure 5a shows a plot which represents the AVM for the blurred data set with different degrees of blurring. Figure 5b shows the AVM for the noisy data set with different degrees of noise. Figure 5c, d shows the AVM for the blurred noisy data set with different degrees of blur and noise. A noticeable improvement could be seen through the plots for the proposed method over the original. Thus, the boundary component involved in affinity improves segmentations with the FC-based method. Further, it can also lessen the effect of poorly defined boundaries as shown in Fig. 4. In this figure, background holes inside the white matter region almost falsely segmented by the original method and merged

with the object region shown in white. On the other hand, the proposed method almost preserves these holes and classifies their spels as background spels.

The second comparison has been performed between the “*proposed threshold*” obtained from Alg. 2 and both the “*poorest threshold*” and “*optimal threshold*.” For each FC scene generated by Alg. 1, these thresholds are identified as indicated in the previous section. With each threshold, the FC scene is segmented by thresholding it; then, we calculate the degree of match for this scene by utilizing Eq. 4.1 and associate this degree with that threshold. Thus, each threshold has a degree of match that expresses the strength of its associated segmentation. Figures 6, 7 and 8 show the degrees of match of the three thresholds (*poorest, proposed, optimal*) involved in segmentation of blurred noisy data set of scenes with different parameters. From these figures, clearly the “*poorest threshold*” and “*optimal threshold*” have the lowest and highest degree of matching as expected. In addition, the “*proposed threshold*” has a degree of match that is much closer to the “*optimal threshold*” degree. Therefore, the “*proposed threshold*” is shown as an appropriate threshold for GFC method.

Table 1 Evaluated measuring percentage for both the original and proposed methods

(a)				
Figure 4a	F-measure	Precision	Recall	Accuracy
Original	95.89	93.07	98.89	99.45
Proposed	96.38	97.76	95.04	0.9954
(b)				
Figure 4d	F-measure	Precision	Recall	Accuracy
Original	0.5345	0.3648	1	0.8959
Proposed	0.5359	0.366	1	0.8965
(c)				
Figure 4g	F-measure	Precision	Recall	Accuracy
Original	0.8802	0.786	1	0.9722
Proposed	0.9185	0.8497	0.9994	0.9819
(d)				
Figure 4j	F-measure	Precision	Recall	Accuracy
Original	0.8492	0.7379	1	0.9704
Proposed	0.8709	0.7713	1	0.9753
(e)				
Figure 4m	F-measure	Precision	Recall	Accuracy
Original	0.9665	1	0.9352	0.9954
Proposed	0.9954	1	0.9908	0.9993

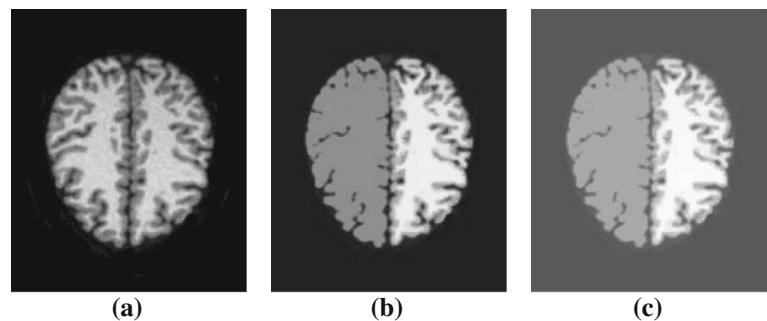
Fig. 9 **a** Ground truth of an image from IBSR, **b** segmented image by the original algorithm, **c** segmented image by the proposed algorithm**Table 2** Evaluated measuring percentage for both the original and proposed methods in IBSR Dataset

Figure 10	F-measure	Precision	Recall	Accuracy
Original	0.5141	1	0.346	0.8784
Proposed	0.5429	1	0.3726	0.8833

As a third comparison, four measures (precision, recall, F-measure and accuracy) have been calculated for the proposed algorithm and the original GFC algorithm (Table 1). All measures have shown that the proposed algorithm is more robust against the noisy and blurred data of the object boundary. In the case of Fig. 10, we used an image from IBSR database, and the corresponding segmentation is shown. Since the proposed and original GFC algorithms are for one object segmentation, the results shown in Fig. 9b, c are presenting one-half of the subject brain image, even the measures values in Table 2 are relatively small for the same reason.

5.2 Ground Truth Versus Proposed

For comparison purpose between the segmented image scene in Fig. 10c and the ground of truth image, a manual mapping of the observations shown in Fig. 10b is utilized. This truth image in Fig. 10b has been created by a geological expert within the collaborative team who delineates the earth observations in the satellite image filed to match with the two different and distinguished concerned areas. The segmented image by the proposed algorithm is shown in Fig. 10c. Matching percentage with the truth image has been calculated. Table 3 shows the number of selected area samples for different used segmentation methods to gather required characteristics of pixels inside the regions needed to segment. Moreover, it shows the percentage of matching between a segmented image scene and the truth image scene.

Fig. 10 **a** Satellite marked image, **b** manual segmented scene (ground truth), **c** segmented image by the proposed algorithm

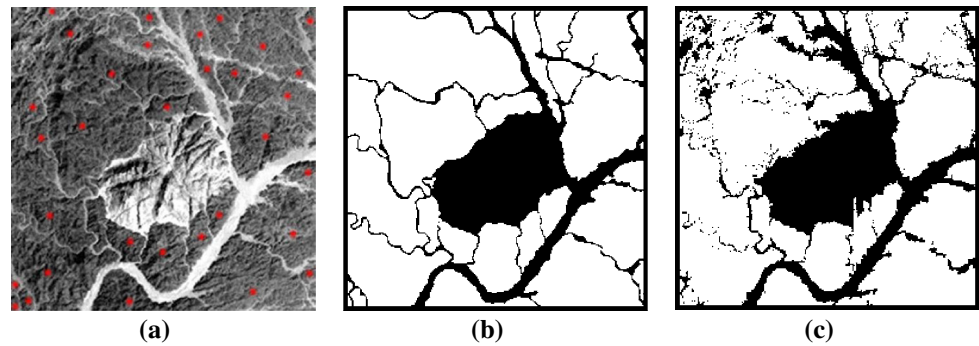


Table 3 Number of selected sample areas for the segmented image by the proposed method and the matching percentage

Method	Selected sample areas	Matching percentage
Proposed	30	91.67%

6 Conclusion

In this article, we introduced a segmentation algorithm based on the absolute FC segmentation method. It modifies the latter method algorithm to tackle some of its weaknesses that affect segmentation accuracy. This algorithm deals with the weakness of “leaking through poorly defined boundary segments” by utilizing boundary-based information in the definition of the local fuzzy relationship (affinity) membership function. Moreover, it automatically determines a threshold parameter for the traditional GFC method to resolve the weakness of specifying it, manually. An evaluation of the proposed algorithm in relation to the traditional GFC algorithm has been performed to assess the suggested modifications. For most cases, an improvement in segmentation of a data set of scenes described above has been shown when applying the proposed algorithm. Specifically, this algorithm eliminates, to some extent, the weakness regarding poorly defined boundaries. In addition, the proposed threshold derived by the algorithm can be considered as a competitive to the optimal threshold.

The proposed algorithm depends on identifying the contour that separates the object to segment from its background, and on the boundary region that separates between them. Therefore, this algorithm is hard to be implemented for scenes having unrecognizable boundaries between objects.

References

- Dougherty, G.: Digital Image Processing for Medical Applications. Cambridge University Press, Cambridge (2009)
- Zaitoun, N.M.; Aqel, M.J.: Survey on image segmentation techniques. *Proced. Comput. Sci.* **65**, 797–806 (2015)
- Parida, P.; Bhoi, N.: Transition region based single and multiple object segmentation of gray scale images. *Eng. Sci. Technol. Int. J.* **19**(3), 1206–1215 (2016)
- Prabha, D.S.; Kumar, J.S.: Performance evaluation of image segmentation using objective methods. *Indian J. Sci. Technol.* **9**(8) (2016). doi:10.17485/ijst/2016/v9i8/87907
- Sonka, M.; Hlavac, V.; Boyle, R.: Image Processing, Analysis, and Machine Vision. Cengage Learning, Boston (2014)
- Rueda, S.; Knight, C.L.; Papageorghiou, A.T.; Noble, J.A.: Feature-based fuzzy connectedness segmentation of ultrasound images with an object completion step. *Med. Image Anal.* **26**(1), 30–46 (2015)
- Saha, P.K.; Udupa, J.K.: Relative fuzzy connectedness among multiple objects: theory, algorithms, and applications in image segmentation. *Comput. Vis. Image Underst.* **82**(1), 42–56 (2001)
- Ciesielski, K.C.; Miranda, P.A.V.; Falcão, A.X.; Udupa, J.K.: Joint graph cut and relative fuzzy connectedness image segmentation algorithm. *Med. Image Anal.* **17**(8), 1046–1057 (2013)
- Udupa, J.K.; Saha, P.K.: Fuzzy connectedness and image segmentation. *Proc. IEEE* **91**(10), 1649–1669 (2003)
- Ciesielski, K.C.; Herman, G.T.; Kong, T.Y.: General theory of fuzzy connectedness segmentations. *J. Math. Imaging Vis.* **55**(3), 304–342 (2016)
- Imielinska, C.; Metaxas, D.; Udupa, J.; Jin, Yinpeng.; Chen, T.: Hybrid segmentation of the visible human data. In: *Proceedings of the Third Visible Human Project Conference*. Citeseer (2000)
- Ciesielski, K.C.; Miranda, P.A.V.; Udupa, J.K.; Falcao, A.X.: Image segmentation by combining the strengths of relative fuzzy connectedness and graph cut. In: *Proceedings of the 19th IEEE International Conference on Image Processing (ICIP), 2012*, pp. 2005–2008. IEEE (2012)
- Jones, T.N.; Metaxas, D.N.: Automated 3D segmentation using deformable models and fuzzy affinity. In: *Proceedings of IPMI97*. Lecture notes in computer science, vol 1230, Springer, Poultny, VT (1997)
- Saha, P.K.; Udupa, J.K.; Odhner, D.: Scale-based fuzzy connected image segmentation: theory, algorithms, and validation. *Comput. Vis. Image Underst.* **77**(2), 145–174 (2000)
- Udupa, J.K.; Samarasekera, S.: Fuzzy connectedness and object definition: theory, algorithms, and applications in image segmentation. *Graph. Models Image Process.* **58**(3), 246–261 (1996)
- Mai, J.K.; Assheuer, J.; Paxinos, G.: Atlas of the Human Brain. Academic Press, San Diego (1997)
- Mai, J.K.; Majtanik, M.; Paxinos, G.: Atlas of the Human Brain. Academic Press, San Diego (2015)
- OBEID, M.; ALI, M.; MOHAMED, N.: Geochemical exploration on the stream sediments of Gabal El Mueilha area, central Eastern Desert, Egypt: An overview on the rare metals. *Resour. Geol.* **51**(3), 217–227 (2001)
- Saha, P.K.; Udupa, J.K.: Iterative relative fuzzy connectedness and object definition: theory, algorithms, and applications in image segmentation. In: *IEEE Workshop on Mathematical Methods in Biomedical Image Analysis, 2000. Proceedings*, pp. 28–35. IEEE (2000)